ELSEVIER

Journal of Chromatography B, 782 (2002) 385–392

JOURNAL OF CHROMATOGRAPHY B

www.elsevier.com/locate/chromb

Peak capacity of ion mobility mass spectrometry: Separation of peptides in helium buffer gas

Brandon T. Ruotolo, Kent J. Gillig, Earle G. Stone, David H. Russell*

Laboratory for Biological Mass Spectrometry, Department of Chemistry, Texas A&M University, College Station, TX 77843, USA

Abstract

Advances in the field of proteomics depend upon the development of high-throughput separation methods. Ion mobility-mass spectrometry is a fast separation method (separations on the millisecond time-scale), which has potential for peptide complex mixture analysis. Possible disadvantages of this technique center around the lack of orthogonality between separation based on ion mobility and separation based on mass. In order to examine the utility of ion mobility-mass spectrometry, the peak capacity (ϕ) of the technique was estimated by subjecting a large dataset of peptides to linear regression analysis to determine an average trend for tryptic peptides. This trend-line, along with the deviation from a linear relationship observed for this dataset, was used to define the separation space for ion mobility-mass spectrometry. Using the maximum deviation found in the dataset ($\pm$11%) the peak capacity of ion mobility-mass spectrometry is ~2600 peptides. These results are discussed in light of other factors that may increase the peak capacity of ion mobility-mass spectrometry (i.e. multiple trends in the data resulting from multiple classes of compounds present in a sample) and current liquid chromatography approaches to complex peptide mixture analysis.

Keywords: Peptides; Helium buffer gas

1. Introduction

The relevance of ion mobility mass spectrometry (IM-MS) to the field of proteomics, where the central challenges include the high throughput analysis of complex mixtures [1] and mapping protein–protein interactions in a proteome [2,3], depends on the analytical utility of IM-MS as compared to current two-dimensional separation methodologies. For any multidimensional separation, such as liquid chromatography–mass spectrometry (LC–MS) or IM-MS, the orthogonality, or the degree of difference between two separation mechanisms [4], of the techniques employed will define the peak capacity (ϕ) of a technique. Peak capacity, or the number of signals that can reside in an area of two-dimensional space [5], is the most common parameter used to evaluate the applicability of a separation method to the analysis of complex mixtures [6]. For example, separation by reversed-phase high-performance liquid chromatography (RP-HPLC), which is based on the partitioning of analytes between a hydrophobic stationary phase and a hydrophilic mobile phase, exhibits good orthogonality to mass measurement (MS) [7]. The high-degree of orthogonality between LC and MS significantly enhances applications of the technique to very complex peptide mixtures because LC–MS disperses signals over a large two-dimen-

*Corresponding author. Tel.: +1-979-845-3345; fax: +1-979-845-9485.

E-mail address: russell@mail.chem.tamu.edu (D.H. Russell).

1570-0232/02/$ – see front matter
PII: S1570-0232(02)00566-4

sional area. This was clearly demonstrated in a recent paper by Shen et al., which reported LC-FTICR peptide separations and an estimated peak capacity of $>6\times10^7$ [7]. As a separation method, ion mobility does not exhibit strict orthogonality to separation based on m/z [8], i.e. a plot of ion mobility drift time for a series of peptides vs. mass-to-charge (m/z) exhibits a near-linear relationship over a limited range (500–2500 m/z). Thus, at this juncture, IM-MS does not possess the peak capacity of LC–MS.

Although IM-MS analysis of peptides using He buffer gas does not demonstrate the same degree of orthogonality as LC–MS, there are strong motivations for developing optimized IM separation methods. For example, ion mobility is a post-ionization separation technique, which enables virtually unlimited sampling of a continually renewed elution profile [9]. On the other hand, LC must be carried out prior to ionization, and this limits the mass analysis to a finite time window defined by the elution profile of an analyte. In addition, the time scale of IM separation, microseconds to milliseconds, more efficiently utilizes the mass spectrometry time scale (microseconds to seconds depending on the method of mass measurement) than does LC, where peptide separation can take several minutes to hours to perform [10]. Separation efficiencies of IM and HPLC, measured in theoretical plates or plate number, are roughly equivalent in most cases [11], and in some cases, the resolution of IM separation has been reported to exceed that of RP-HPLC [12]. Until recently, high-resolution IM separation has suffered from low limit of detection (LOD) and sensitivity [9]; however, periodic focusing ion mobility drift cell technology has been shown to extend the LOD for IM-MS to femtomolar amounts of material [13].

The drift time of an ion (K^{-1}) depends directly on the collision cross-section of the ion (Ω) and the reduced mass of the ion-neutral collision complex (μ), and inversely upon the charge carried by the ion (z) [14]. For large ions ($M_w>$approximately 500), using helium as the buffer gas, the ion–neutral interaction potential can be assumed to be negligible. In addition, as the molecular mass of the ion increases, the reduced mass of the ion–neutral collision partners is essentially constant and can be ignored, resulting in a separation based exclusively on the collision cross-section [15]. In other words, there is direct proportionality between K^{-1} and Ω for mobility separations of identically charged, large, homologous ions.

If differences in conformation, charge, and chemical class are ignored, then it is reasonable to assume that as an ion increases in mass it will also increase in overall collision cross-section [16]. Thus, noting the established relationship between K^{-1} and Ω, there is by extension a proportional relationship between K^{-1} and the mass of the ion. This proportionality is observed in plots of drift time vs. m/z (mobility–mass plot) as a near-linear trend over a limited mass range for a single ion series (500–3000 m/z for singly-charged peptide ions). The approximations made thus far do not consider differences in gas-phase conformation, which can result in deviations from the linear mass–mobility relationship [17,18]. If a particular peptide ion can exist as two distinct conformers due to intramolecular interactions such as hydrogen bonding, proton bridges, or salt-bridges, collision cross-sections of the different conformers may differ and signals for the individual conformers may be observed as distinct peaks [19]. On the other hand, if the peptide exists as many conformers, or as two (or more) interconverting conformers, this can give rise to signal broadening and a loss of resolution [20].

In chromatographic terms, the peak capacity (ϕ) is defined as the greatest possible number of individual analytes that can be separated by a technique [5]. Peak capacity is therefore a function of the resolution of a method. In the case of a two-dimensional technique, ϕ is also a function of the degree of difference between (orthogonality of) the two separation methods employed. Because there is a near-linear relationship between drift time and m/z (for a homologous series of ions), the variability, i.e. conformational differences, of a given set of molecules can be used to determine ϕ for IM-MS separation. This approach is illustrated in Fig. 1, which is a schematic diagram of a mobility–mass plot. Hypothetically, if there were a strict linear correlation between drift time and m/z the plot shown in Fig. 1 would contain no shaded area, i.e. signals could only appear along the best-fit line. On the other hand, if there was complete orthogonality

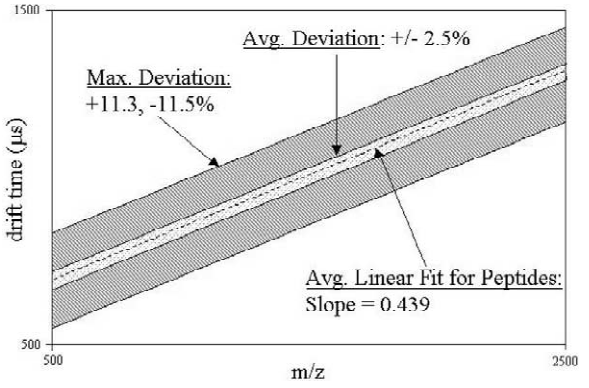

Fig. 1. Schematic diagram of the observed separation space for IM-MS. The centerline represents the average mobility–mass trend-line for peptides. The first lightly shaded area is the separation window based on the average peptide deviation. The second, larger area is based on the maximum deviation observed for peptide ions.

between the separation mechanisms employed, then the shaded area in Fig. 1 would encompass the entire two dimensional plot and signals could appear anywhere in separation space. IM-MS separation presents a case that is in-between the two extremes. Peak capacity calculations are carried out by defining a two-dimensional area (separation window) within which IM-MS separation of peptides takes place. The area of this 2-D space is calculated in terms of peaks, i.e. the resolution of the two dimensions are used to convert the units of each dimension to that of a hypothetical peak. Therefore, for a two-dimensional technique (such as IM-MS) the ϕ value would be given by

$$\phi = (L_1/\Delta t_{\mathrm{avg1}})(L_2/\Delta t_{\mathrm{avg2}}) \quad (1)$$

where L is the length (for IM-MS L is given in either mass or drift time) of a given dimension of the separation, and Δt_{avg} is the average width of a peak at half-height, defined as the average of the peak widths at half height for the extremes of a given range [5]. This work will focus on our recent efforts to chart the peak capacity and orthogonality of IM separation as applied to peptide analysis, and evaluate the utility of ion mobility separation of peptide ions. The following discussion considers the peak capacity of IM-MS for the separation of peptides of m/z 500–2500 (typical mass range for tryptic peptides ionized by MALDI) in He buffer gas.

2. Experimental

Experiments were carried out on a MALDI-IM-oTOF-MS instrument described elsewhere [13]. Briefly, ions are formed by matrix assisted laser desorption–ionization (MALDI) (at 337 nm) at the operating pressure of the drift cell (1–10 Torr He) and drift through a periodic focusing ion mobility drift tube on the millisecond time scale (drift times range from 0.5 to 1.5 ms for peptide separations). Ions eluting from the drift cell are then sampled and mass identified by an orthogonal time-of-flight mass spectrometer (o-TOF). Protein digest samples were prepared utilizing proteins purchased from Sigma (St. Louis, MO, USA.), utilizing a 40:1 substrate to enzyme ratio and thermal denaturation as discussed previously [21] using stock solutions of α-casein (bovine), β-casein (bovine), serum albumin (bovine), hemoglobin (bovine), myoglobin (horse heart), phosphorylase (rabbit), aldolase (rabbit), ovalbumin (chicken egg), lysozyme (chicken egg white), cytochrome c (horse heart), apo-transferrin (bovine), carbonic anhydrase (bovine), ubiquitin (bovine) all purchased from Sigma and used without additional purification. In addition a dataset of model peptides, discussed in detail elsewhere, was included for these calculations [22]. Sample preparation [23] involved the dilution of the resulting 10 pmol/ml solution with α-cyano-4-hydroxy cinnamic acid to a matrix to analyte ratio of 1000:1. The sample was then spotted on the probe tip and inserted into the source of the instrument with no additional clean-up or preparation. In-source decay (ISD) fragmentation for DNA/peptides and carbon cluster formation are achieved by increasing the ionizing laser power to levels exceeding the threshold for ion formation [24].

Linear regression analysis was performed using CURVE EXPERT (Microsoft, Seattle, WA, USA). Separate fits were performed on all 14 datasets, the average of these separate fits were used to define the average best-fit line. Datasets consist of centroid mass and centroid mobility values for all identified ion signals within the 14 spectra, i.e. no unidentified/unknown peaks were used in calculations of theoretical ϕ values. Data points were not compiled into a single dataset and fit due to small run-to-run variations in experimental conditions. This approach does not consider the contributions of slope variations in

the digest spectra (which varied from 0.330 to 0.547), and deals with only the overall observed spread of the data from a single normalized trendline. The slope of the average best-fit line was 0.439, and the average correlation coefficient was 0.991. The average best-fit line for the 14 separate fits and the maximum deviation of IM-MS peptide ion signals was used to define the 2-D separation window for calculations of theoretical ϕ values. Deviations from linear relationships are reported relative to the corrected drift time of the ion in question[1].

3. Results and discussion

Fig. 2 contains a mobility–mass plot (a plot of drift time vs. m/z) for a series of singly charged peptide ions. Note that over a limited mass range the mobility–mass plot is nearly linear. Utilizing database searching [26], 35 tryptic peptides from rabbit muscle phosphorylase were identified from Fig. 2 based on m/z measurement alone. The deviations from a best-fit linear relationship for observed ion signals range from ±5% to ±0.1% in drift time, with

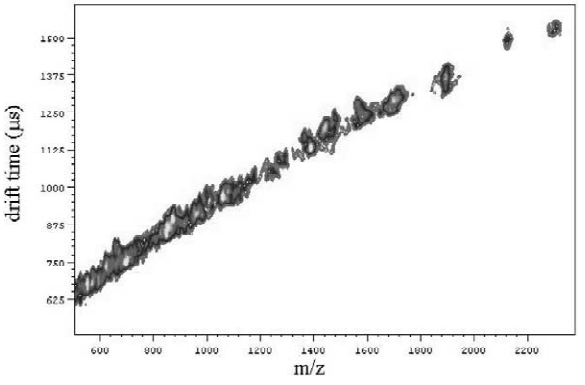

Fig. 2. Example mobility–mass plot of one of the 14 datasets presented, a tryptic digest of rabbit muscle phosphorylase.

[1]Instrumental drift time was corrected for transit time through the lens system that links the ion mobility drift tube to the orthogonal time-of-flight source according to the following equation: $t = 72.20 \times \{[(m/z)^{1/2} \times l]/V^{1/2}\}$ where t is the transit time through the lens, m is the mass of the ion, z is the charge of the ion, l is the length of the lens (in this case 0.209 m), and V is the voltage on the accelerating element of the lens. Instrument Diagrams are available in Ref. [13].

an average absolute deviation for the entire dataset of 0.12% drift time. The variation from a linear relationship on the mass–mobility plot is typical of MALDI-IM-MS peptide maps of tryptic protein digests.

Fig. 3A (a residual plot) and 3B (a summary histogram) illustrate the deviation for a much larger dataset of peptide ions. These data were obtained from linear regression analysis of 14 separate datasets, similar to that shown in Fig. 2. Each individual dataset is either one of thirteen digested proteins or a mixtures of model peptides. Overall, the dataset contains a wide variety of sequences, including post-translational modifications (threonine and serine phosphorylation only). The deviation from strictly linear mobility–mass plot for these peptides ranged between ±11% (maximum) and ±0.1 (minimum) in drift time. The overall average deviation for the dataset was ±2.5% drift time. It is important to note that the maximum deviation is due to large differences in gas-phase conformation within the peptide dataset ranging from helical peptides, which exhibit large positive deviation from a linear relationship, to extensively folded peptides, which exhibit large negative deviation [17].

If we calculate the theoretical peak capacity (ϕ), using Eq. (1), for IM-MS using the maximum deviation from a linear fit (±11%), assuming a constant mobility resolution of 60 and a constant mass resolution of 400 for all peptides separated, we obtain a value of ~2600. The calculated peak capacity represents a five-fold increase in the peak capacity of the mass spectrometer alone (530 peaks over a m/z range of 500–2500 at a resolution of 400). If a similar calculation is performed, using the average deviation of the dataset (±2.5% in drift time) ϕ is found to be ~530. In this case the two-dimensional space defined by the average deviation from a strictly linear mobility–mass plot is large enough to contain one signal with a mobility resolution of 60, and thus yields a ϕ value equivalent to MS separation alone (see Fig. 1).

Several assumptions are made in order to estimate ϕ for He-based IM-MS separation. First we assume that the resolution of both techniques is constant for all ions. This assumption does not generally hold true for any separation technique and is commonly referred to as the ''general elution problem'' [6].

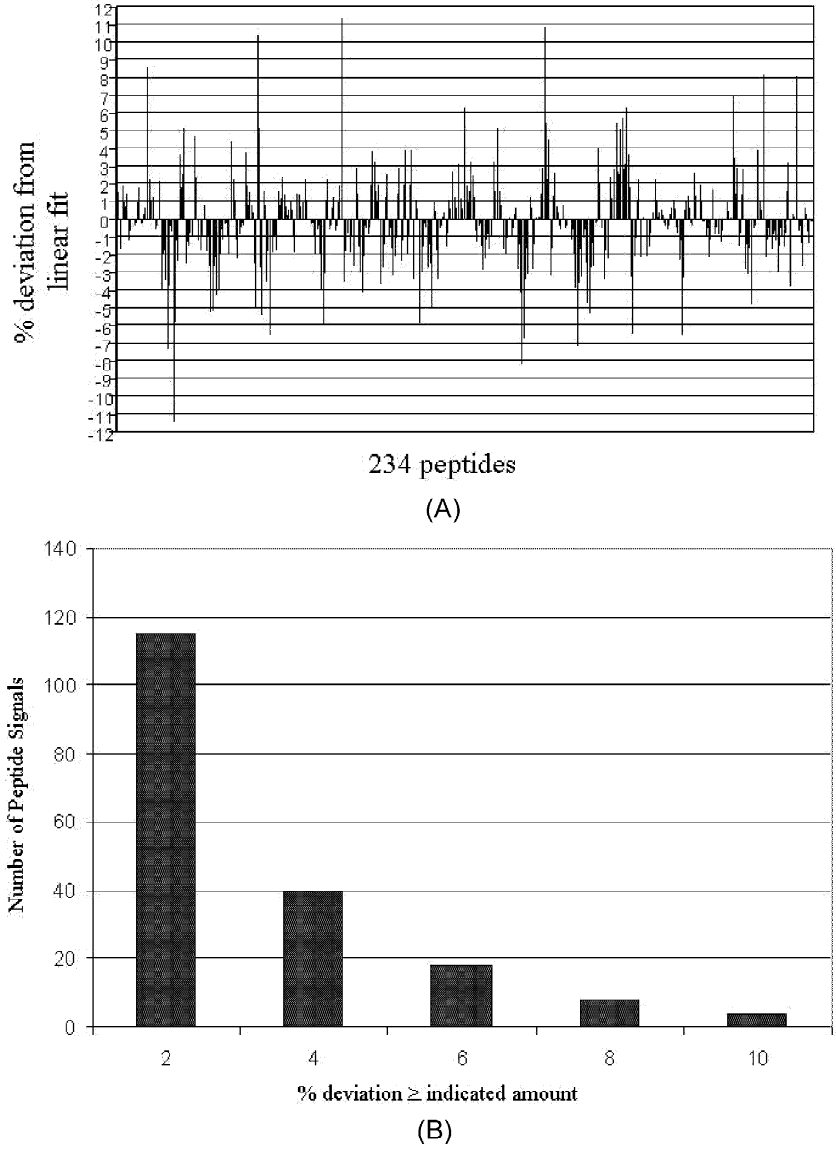

Fig. 3. (A) Plot of the residuals (in% deviation from the drift time predicted by the fit for a particular peptide ion observed) for 14 separate linear regression fits of the peptide datasets. (B) Histogram plot summarizing (A). The number of signals observed having greater than or equal to the percentage deviation indicated is given for 5 selected deviation values (2, 4, 6, 8 and 10).

This is not a variable that can be accounted for based on the simplified framework outlined in this paper, thus the estimate produced should be regarded as a slight overestimate of the practical peak capacity. Second, we assume that the peptide dataset is an adequate sampling of the range of deviations from a linear relationship between drift time and m/z for peptide ions formed by MALDI and separated in He. Due to the variability of the sequences represented and the number of peptides in the dataset presented in Fig. 3, we feel that the current dataset of 234 peptides is sufficient for the purposes of estimation.

The preceding discussion took only peptide ions into consideration. However, data has also been

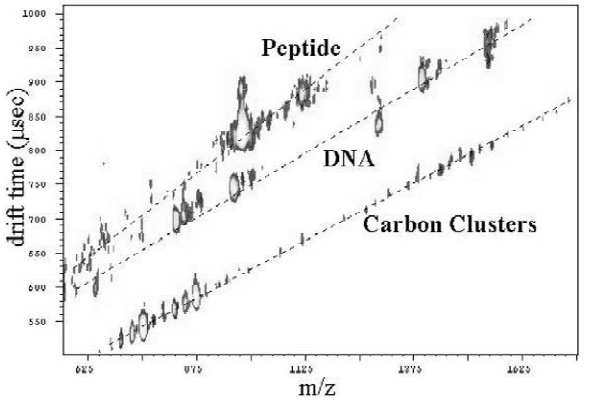

Fig. 4. Mobility–mass plot of a complex mixture containing multiple classes of ions. In this case peptide, DNA, and carbon cluster ions are observed. Lines are superimposed onto the plot to indicate the mobility–mass trends for each class of molecule.

acquired for mixtures of different classes of compounds. For example, Fig. 4 shows the difference in mobility–mass relationship for peptide, DNA, and carbon cluster (C_{60} related) ions. Fullerene derived carbon clusters are more compact in the gas-phase when compared to peptide and DNA ions of similar mass, making carbon cluster signals discernable from peptide signals [23]. Similarly, DNA ions including in-source decay (ISD) fragment ions of the 5-mer GGATC are also more compact than peptide ions in the gas-phase [27]. In all cases IM-MS is able to separate the peptide ions from the ions originating from DNA and carbon clusters.

The ϕ value derived for complex mixtures containing more than one class of molecule are higher than that estimated for single homologous ion series. If it is assumed that peptide signals are completely separated from the other signals, as shown in Fig. 4, ϕ of the second series of ions (DNA or carbon cluster) is a function of the variation of the ions from a strictly linear mobility–mass plot, and the total peak capacity of a composite sample is simply the sum of the ϕ values for the two separations. In the case of C_{60} carbon clusters, where little deviation is observed (in the limited mass range shown in Fig. 4) the additional peak capacity would be the ϕ value for the mass spectrometer (an additional 530 peaks for the mass spectrometer used in these studies). For DNA signals, which exhibit an overall variation of $+8\%/-5\%$ (from linear regression) based on the composition (of ISD fragment ions) and gas-phase conformation [26], the ϕ value increases to ~1280 peaks. However, it should be noted that, based on our more extensive database of peptide ion mobility behavior, there are some cases where the separation windows for peptide and DNA ions overlap. Thus, the peak capacity of such complex mixture separations is a function of the resolution of the separation, the respective separation windows for each compound, and the overlap of the separation windows for the ions observed. In general, based on the evidence presented in Fig. 4 and calculations utilizing Eq. (1), ϕ values for IM-MS increases by a factor of 1.2 or greater when additional chemical classes of components are added to a sample, and such separations demonstrate the true potential for the application of IM-MS to unknown mixtures.

4. Conclusion

Although IM-MS separations do not possess the peak capacity of LC–MS techniques at this point, ϕ is high enough to be useful in most cases even when considering complex mixtures of protein digests (~10 proteins or >100 peptide signals) and has the added advantage over liquid based methods of a more efficient use of the mass spectrometry timescale. Results suggest that the true peak capacity of IM-MS (using He buffer gas) lies between 1 and 5 fold increase in the peak capacity of MS alone. Previously, we reported that IM-MS, as a tandem technique, has an intrinsically higher dynamic range than single stage mass spectrometry [23]. This added dynamic range undoubtedly accounts for some portion of the increased peak capacity of IM-MS over stand alone MS. In those cases when the sample contains two or more types of biological material, IM-MS analysis has a greater theoretical ϕ than for a single component IM-MS separation. Although it was not discussed here, a limited amount of data indicates that an analysis of a complex mixture that includes post-translationally modified peptides may exhibit increased peak capacity over separations that do not include modified peptides [22,28]. In addition, ESI-IM data has shown that multiply charged peptide ions can exist on trend-lines somewhat removed from that of singly charged peptide ions [29], thus

providing an increased 2-D separation space for peptide ions [30] and increasing the possibility of overlap between peptide ions and other classes of molecules (i.e. DNA).

The challenge of separation–mass spectrometry in the era of proteomics is high-throughput separations, and IM-MS provides a higher throughput separation alternative relative to liquid based separation methods. The throughput advantage of IM-MS can be illustrated by comparing techniques in terms of peak capacity per unit time (i.e. ϕ/s). For example, the ϕ/s value for the LC–FTICR separation reported by Shen et al. [7] is approximately 12 500 (6×10^7 peaks acquired over ~4800 s), while the IM-MS ϕ/s value is 1.3×10^6 (2600 peaks acquired over 0.002 s).

There are several steps that can be taken to increase the performance of both IM and MS. High-resolution IM (resolution >100) separations in He coupled to a high resolution TOF MS (resolution ~5000), would make it possible to detect tens of thousands of peptide signals (using Eq. (1)). The data content of IM-MS can be expanded even further by incorporating a dissociation step prior to mass analysis, and acquiring drift-time correlated fragment ion spectra [31,32]. Such IM-MS–MS methods can disperse both fragment ions and parent ions in a single two-dimensional plot, thus increasing the effective peak capacity of the technique. It is important to emphasize that this peak capacity increase, as it is derived from ion fragmentation and does not further disperse primary (parent) ions in separation space, does not provide a concomitant increase in utility for complex mixture analysis. Lastly, Hill et al. [33] have clearly shown that changes in bath gas composition can affect the selectivity (α) of an ion mobility separation. In order to handle samples that require a higher ϕ value, we plan to utilize binary gas mixtures to enhance the influence of the ion-neutral interaction term of the collision cross-section, and thereby increase ϕ further.

Acknowledgements

The authors thank Dr. John Mclean and Holly Sawyer for their comments. This work is supported by the National Science Foundation (CHE-9629966) and by the Department of Energy, Division of Chemical Sciences BES (DE-FG03-95ER14505).

References

[1] M.P. Washburn, D. Wolters, J.R. Yates, Nature Biotechnol. 19 (2001) 242.
[2] Y. Ho, A. Gruhler, A. Hellbut, G.D. Bader, L. Moore, S. Adams, A. Millar, P. Taylor, K. Bennett, K. Boutiller, L. Yang, C. Wolting, I. Donaldson, S. Schandorff, J. Shewnarane, M. Vo, J. Taggartt, M. Goudreault, B. Muskat, C. Alfarano, D. Dewar, Z. Lin, K. Michallckova, A.R. Willems, H. Sassi, P.A. Nielsen, K.J. Rasmussen, J.R. Andersen, L.E. Johansen, L.H. Hansen, H. Jespersen, A. Podtelejnikov, E. Nielsen, J. Crawford, V. Poulsen, B.D. Sorensen, J. Matthlesen, R.C. Hendrickson, F. Gleeson, T. Paweson, M.F. Moran, D. Durocher, M. Mann, C.W. Matthias, V. Hogue, D. Figeys, M. Tyers, Nature 415 (2002) 180.
[3] A.-C. Gavin, M. Bosche, R. Krause, P. Grandi, M. Marzloch, A. Bauer, J. Schultz, J.M. Rick, A.-M. Michon, C.M. Cruclat, M. Remor, C. Hofert, M. Schelder, M. Brajenovlc, H. Ruffner, A. Merino, K. Klein, M. Hudak, D. Dickson, T. Rudi, V. Gnau, A. Bauch, S. Bastuck, B. Huhse, C. Leutweln, M.-A. Heurtier, R.R. Copley, A. Edelmann, E. Querfurth, V. Rybin, G. Drewes, M. Raida, T. Bouwmeester, P. Bork, B. Seraphin, B. Kuster, G. Neubauer, G. Superti-Furga, Nature 415 (2002) 141.
[4] D.J. Rose, G.J. Opiteck, Anal. Chem. 66 (1994) 2529.
[5] J.C. Giddings, Anal. Chem. 56 (1984) 1258A.
[6] B.L. Karger, L.R. Snyder, C. Horvath, in: An Introduction To Separation Science, Wiley, New York, 1973, p. 155.
[7] Y. Shen, N. Tolic, R. Zhao, L. Pasa-Tolic, L. Li, S.J. Berger, R. Harkewicz, G.A. Anderson, M.E. Belov, R.D. Smith, Anal. Chem. 73 (2001) 3011.
[8] E.A. Mason, in: T.W. Carr (Ed.), Plasma Chromatography, Plenum Press, New York, 1984, p. 43.
[9] K.J. Gillig, B. Ruotolo, E.G. Stone, D.H. Russell, K. Fuhrer, M. Gonin, A.J. Schultz, Anal. Chem. 72 (2000) 3965.
[10] J.F. Holland, C.G. Enke, J. Allison, J.T. Stults, J.D. Pinkston, B. Newcome, J.T. Watson, Anal. Chem. 55 (1983) 997A.
[11] G.R. Asbury, H.H. Hill, J. Microcol. Sep. 12 (2000) 172.
[12] P. Dugourd, R.R. Hudgins, D.E. Clemmer, M.F. Jarrold, Rev. Sci. Instrum. 68 (1997) 1122.
[13] K.J. Gillig, D.H. Russell, PCT Int. Appl. (2001) WO 0165589.
[14] E.W. McDaniel, E.A. Mason, in: The Mobility and Diffusion of Ions in Gases, Wiley, New York, 1973, p. 68.
[15] A.A. Shvartsburg, M.F. Jarrold, Chem. Phys. Lett. 261 (1996) 86.
[16] P.D. Mosier, A.E. Counterman, P.C. Jurs, D.E. Clemmer, Anal. Chem. 74 (2002) 1360.
[17] A.E. Counterman, D.E. Clemmer, J. Am. Chem. Soc. 123 (2001) 1490.
[18] B.T. Ruotolo, G.F. Verbeck, L.M. Thomson, K.J. Gillig, D.H. Russell, J. Am. Chem. Soc. 124 (2002) 4214.

[19] D.E. Clemmer, M.F. Jarrold, J. Mass Spectrom. 32 (1997) 577.
[20] C. Wu, W.F. Siems, J. Klasmeier, H.H. Hill, Anal. Chem. 72 (2000) 391.
[21] Z.-Y. Park, D.H. Russell, Anal. Chem. 72 (2000) 2667.
[22] B.T. Ruotolo, G.F. Verbeck IV, L.M. Thomson, A.S. Woods, K.J. Gillig, D.H. Russell, J. Proteome Res. 1 (2002) 303.
[23] B.T. Ruotolo, K.J. Gillig, E.G. Stone, D.H. Russell, K. Fuhrer, M. Gonin, J.A. Schultz, Int. J. Mass Spectrom. 219 (2002) 253.
[24] R.J. Cotter, Time-of-flight mass spectrometry: instrumentation and applications, in: Biological Research, American Chemical Society, Washington, DC, 1997, p. 162.
[26] http://prospector.ucsf.edu/.
[27] J.M. Koomen, B.T. Ruotolo, K.J. Gillig, J.A. Mclean, M. Kang, K. Fuhrer, M. Gonin, J.A. Schultz, K.R. Dunbar, D.H. Russell, J. Anal. Bioanal. Chem. 373 (2002) 612.
[28] J.M. Kindy, J.A. Taraszka, F.E. Regnier, D.E. Clemmer, Anal. Chem. 74 (2002) 950.
[29] S.J. Valentine, A.E. Counterman, C.S. Hoaglund, J.P. Reilly, D.E. Clemmer, J. Am. Soc. Mass Spectrom. 9 (1998) 1213.
[30] S.J. Valentine, M. Kulchania, C.A. Srebalus-Barnes, D.E. Clemmer, Int. J. Mass Spectrom 212 (2001) 97.
[31] C.S. Hoaglund-Hyzer, J. Li, D.E. Clemmer, Anal. Chem. 73 (2000) 2737.
[32] E.G. Stone, K.J. Gillig, B.T. Ruotolo, D.H. Russell, Int. J. Mass Spectrom. 212 (2001) 519.
[33] G.R. Asbury, H.H. Hill, Anal. Chem. 72 (2000) 580.